



Numerical study of the effect of a charged membrane in the separation of electrically charged components

S.I.S. Pinto^a, J.M. Miranda^{b*}, J.B.L.M. Campos^a

^a*Centro de Estudos de Fenómenos de Transporte, Departamento de Engenharia Química, Faculdade de Engenharia da Universidade do Porto, Rua Dr. Roberto Frias, 4200-465 Porto Portugal*

^b*Universidade Lusófona do Porto, Rua Augusto Rosa, n° 24, 4000-098 Porto, Portugal*
Fax: +351 225081692, email: jmiranda@gmail.com

Received 30 June 2009; accepted 4 November 2009

ABSTRACT

The efficiency of protein fractionation by ultrafiltration is reduced by concentration polarization, which indirectly reduces the apparent selectivity of the membrane. The complete understanding of this phenomenon requires the knowledge of the electrical interactions between the membrane and the solutes. These interactions are studied by numerical methods. A numerical code, based on a finite volume method, is developed to study the separation of a solution containing two charged solutes by solving the Poisson-Boltzmann, the Navier-Stokes and the Nernst-Planck equations. The code is used to study the effects of the electric charge of the membrane in the concentration fields of the solutes.

Keywords: Numerical methods; Electrically charged membranes; Membrane separation processes; Nernst-Planck equation; Poisson-Boltzmann equation

1. Introduction

In protein fractionation by ultrafiltration, mass accumulates near the surface of the membrane, given rise to the so called concentration polarization phenomenon. Concentration polarization reduces the permeability and the selectivity of the process [1–3]. It is known that concentration polarization can be influenced by the physicochemical conditions near the membrane [4–6]. The effect of physicochemical conditions is due to ion-ion, membrane-ion, protein-ion, protein-protein [7] and membrane-protein interactions. Molecular and ionic interactions can be dealt with by modeling their effects on the diffusivity of the components and on the osmotic pressure of the solution [4,5].

However, membrane-ion and membrane-protein interactions deserved relatively less attention by researchers. Analytical and numerical methods developed so far can capture the effects of concentration dependent properties [8,9], multicomponent diffusion [10] and convection-diffusion across the membrane [11,12]. Electrical interactions between the membrane and charged components are usually neglected in most studies. However, in some separation processes, they cannot be ignored.

Here, we cover the modeling of the interactions between the membrane surface and charged components by solving numerically the electric potential equation and the flow and mass transport equations in the separation cell. Our interest is to study the separation of a solution of two species with opposite charges by a charged membrane in a parallel plate membrane cell.

*Corresponding author

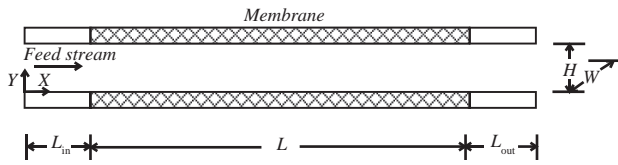


Fig. 1. Cell.

2. Cell description

The cell under study is schematically represented in Fig. 1. It is a parallel plate cell with a permeable membrane on both sides. The distance between the plates, H , is 10^{-3} m. The width and length of the cell are W and L , respectively. The inlet (L_{in}) and outlet (L_{out}) sections are both impermeable to the solutes and to the solvent.

The feed stream is separated into two streams: the retentate stream which is richer in the charged species, and the permeate stream which is richer in the solvent. The membrane has a negative zeta potential (ranging between $\phi_w = -1$ mV and $\phi_w = -10$ mV [13]) and a resistance of 5.714×10^9 kg m⁻² s⁻¹. The feed stream is a diluted ionic solution ($C_0^+ = 1 \times 10^{-5}$ mol m⁻³ and $C_0^- = 1 \times 10^{-5}$ mol m⁻³).

3. Theory

To model the flow and mass transport in the cell, the following simplifications were considered:

- The solutes are completely rejected by the membrane;
- The osmotic pressure can be neglected;
- The physical properties are constant (viscosity of the solution and diffusivity of the solutes);
- The electric field is determined based on the Boltzmann distribution of charged components. Effects of convection in the electric field are considered negligible;
- Electric effects on the flow are neglected.

To study the effect of the electric interactions in the concentration at the membrane surface, it is necessary to determine the electric field, the concentration field and the flow field. Therefore, the Poisson-Boltzmann, the Navier-Stokes equations and the Nernst-Planck equation were solved. Although only steady state results are presented, the numerical method is based on the solution of the transient equations. The equations were solved in the numerical domain represented in Fig. 2. The numerical domain represents half of the

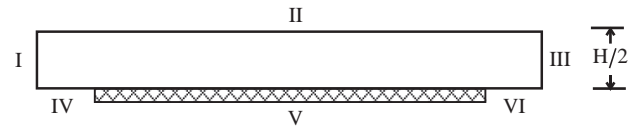


Fig. 2. Numerical domain.

physical cell (the cell is symmetric) and comprises an inlet section, an outlet section and the membrane.

4. Electric Potential Equation

The electric potential follows the Poisson-Boltzmann equation:

$$\frac{\partial \phi}{\partial t} = \left(\frac{\partial^2 \phi}{\partial x^2} + \frac{\partial^2 \phi}{\partial y^2} \right) - \Pi_2 r_e \quad (1)$$

where ϕ is the electric potential normalized by the membrane potential (Φ_w), r_e is the ionic concentration and Π_2 is defined by:

$$\Pi_2 = \frac{FC_0H^2}{\varepsilon M\Phi_w} \quad (2)$$

where F is the Faraday constant, C_0 the feed concentration, M the mean molar mass of the species in solution and ε the permittivity.

The normalized ionic concentration is the algebraic sum of the individual ionic concentrations:

$$r_e = \sum_{i=1}^N z_i c_i \quad (3)$$

where z_i is the electric charge number and c_i the normalized (by the feed concentration) concentration of component i .

Considering the approximation of negligible convection in both directions (X and Y), the normalized concentration of the components are related to the electric field through the Boltzmann distribution:

$$c_i = c_0 \exp[-z_i \Pi_3 (\phi - \phi_0)] \quad (4)$$

where c_0 is the normalized concentration of the component in the bulk (far from the membrane), ϕ_0 the non-dimension electric potential in the bulk, and Π_3 a dimensionless number defined by:

$$\Pi_3 = \frac{F\Phi_w}{RT} \quad (5)$$

Combining Eq. 3 and Eq. 4, the normalized ionic concentration can be related with the electric field by:

$$r_e = -2 \sinh[\Pi_3(\phi - \phi_0)] \quad (6)$$

Combining all the previous equations, the Poisson-Boltzmann becomes:

$$\frac{\partial \phi}{\partial t} = \left(\frac{\partial^2 \phi}{\partial x^2} + \frac{\partial^2 \phi}{\partial y^2} \right) + 2\Pi_2 \sinh[\pi_3(\phi - \phi_0)] \quad (7)$$

To solve the Poisson-Boltzmann equation by numerical methods, boundary conditions must be specified at the boundaries of the domain. At the membrane surface ($z = 0$), non-dimensional electric potential is:

$$\phi = \frac{\Phi_w}{\Phi_w} = 1 \quad (8)$$

At the axis of symmetry the variation of the non-dimensional electric potential along the normal direction is equal to zero:

$$\frac{\partial \phi}{\partial y} = 0 \quad (9)$$

At the cell inlet and at the cell outlet the variation of the non-dimensional electric potential along the normal direction is also equal to zero:

$$\frac{\partial \phi}{\partial x} = 0 \quad (10)$$

The Poisson-Boltzmann was solved by a finite difference method. The second derivatives were approximated by implicit central differences and the non-linear term was taken explicitly.

4.1. Flow Equations

The flow is described by the Navier-Sokes equations. For a bi-dimensional cell, the Navier-Sokes equation can be written for secondary variables (vorticity, ω , and stream function, ψ) as the vorticity transport equation and a Poisson equation. For Cartesian coordinates (x and y), the vorticity transport equation is:

$$\frac{\partial \omega}{\partial t} + v_x \frac{\partial \omega}{\partial x} + v_y \frac{\partial \omega}{\partial y} = \frac{1}{\text{Re}} \left(\frac{\partial^2 \omega}{\partial x^2} + \frac{\partial^2 \omega}{\partial y^2} \right) - \Pi_1 \left(\frac{\partial r_e}{\partial y} \frac{\partial \phi}{\partial x} - \frac{\partial r_e}{\partial x} \frac{\partial \phi}{\partial y} \right) \quad (11)$$

where Π_1 is a non - dimensional number given by:

$$\Pi_1 = \frac{FC_0 \Phi_w}{M \rho V_0^2} \quad (12)$$

where ρ is the fluid density and V_0 the feed velocity.

The Reynolds number (Re), based on the height of the parallel plate cell, is given by:

$$\text{Re} = \frac{\rho V_0 H}{\mu} \quad (13)$$

Considering that the variation of the electric potential along the horizontal direction is negligible and that r_e changes slowly along x , as first approximation, the electric term of the vorticity equation can be neglected:

$$-\Pi_1 \left(\frac{\partial r_e}{\partial y} \frac{\partial \phi}{\partial x} - \frac{\partial r_e}{\partial x} \frac{\partial \phi}{\partial y} \right) = 0 \quad (14)$$

The Poisson equation for the stream function is:

$$\omega = \frac{\partial^2 \psi}{\partial x^2} + \frac{\partial^2 \psi}{\partial y^2} \quad (15)$$

The velocity components are related to the stream function by:

$$v_x = \frac{\partial \psi}{\partial y}; \quad v_y = \frac{\partial \psi}{\partial x} \quad (16)$$

When the osmotic pressure of the solution can be neglected, the velocity boundary condition at the membrane surface is:

$$v_z = \frac{\Delta P_0}{R_m V_0} \quad (17)$$

where ΔP_0 is the transmembrane pressure and V_0 the feed velocity. The remaining boundary conditions and the numerical methods to solve the vorticity transport equation and the Poisson equation are presented in [10].

5. Mass transport equations

The mass transport equation, for each component, is:

$$\frac{\partial c_i}{\partial t} + \frac{\partial (v_x c_i)}{\partial x} + \frac{\partial (v_y c_i)}{\partial y} = \frac{1}{\text{Pe}_i} \left(\frac{\partial^2 c_i}{\partial x^2} + \frac{\partial^2 c_i}{\partial y^2} \right) + \left[\frac{\partial \left(\frac{z_i \Pi_3}{\text{Pe}_i} c_i \frac{\partial \phi}{\partial x} \right)}{\partial x} + \frac{\partial \left(\frac{z_i \Pi_3}{\text{Pe}_i} c_i \frac{\partial \phi}{\partial y} \right)}{\partial y} \right] \quad (18)$$

where Pe_i is the Peclet number:

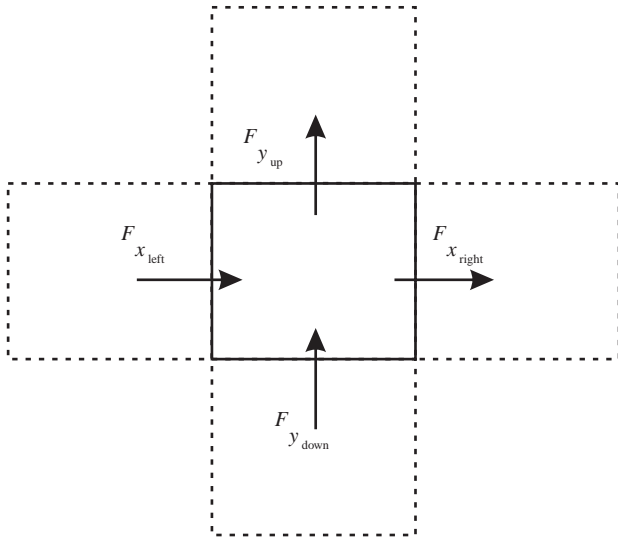


Fig. 3. Mass fluxes across the boundaries of a finite volume.

$$Pe_i = \frac{V_0 H}{D_i} \quad (19)$$

In this definition D_i is the diffusivity of component i .

The electric and convective terms of equation 18 can be grouped:

$$\begin{aligned} \frac{\partial c_i}{\partial t} + \frac{\partial \left[\left(v_x - \frac{z_i \Pi_3}{Pe_i} \frac{\partial \phi}{\partial x} \right) c_i \right]}{\partial x} + \frac{\partial \left[\left(v_y - \frac{z_i \Pi_3}{Pe_i} \frac{\partial \phi}{\partial y} \right) c_i \right]}{\partial y} \\ = \frac{1}{Pe_i} \left(\frac{\partial^2 c_i}{\partial x^2} + \frac{\partial^2 c_i}{\partial y^2} \right) \end{aligned} \quad (20)$$

Defining the following variables:

$$\hat{v}_x = \left(v_x - \frac{z_i \Pi_3}{Pe_i} \frac{\partial \phi}{\partial x} \right) \quad (21)$$

$$\hat{v}_y = \left(v_y - \frac{z_i \Pi_3}{Pe_i} \frac{\partial \phi}{\partial y} \right) \quad (22)$$

Equation 20 can be simplified:

$$\frac{\partial c_i}{\partial t} + \frac{\partial(\hat{v}_x c_i)}{\partial x} + \frac{\partial(\hat{v}_y c_i)}{\partial y} = \frac{1}{Pe_i} \left(\frac{\partial^2 c_i}{\partial x^2} + \frac{\partial^2 c_i}{\partial y^2} \right) \quad (23)$$

The terms $\frac{\partial(\hat{v}_x c_i)}{\partial x}$ and $\frac{\partial(\hat{v}_y c_i)}{\partial y}$ are pseudoconvective terms that, from the numerical point of view, can be solved by methods designed to solve convection terms. The mass transport equation was solved by a fractional-step method [14], with the pseudoconvective terms separated from the diffusive terms:

$$\frac{\partial c_i}{\partial t} + \frac{\partial(\hat{v}_x c_i)}{\partial x} + \frac{\partial(\hat{v}_y c_i)}{\partial y} = 0 \quad (24)$$

$$\frac{\partial c_i}{\partial t} = \frac{1}{Pe_i} \left(\frac{\partial^2 c_i}{\partial x^2} + \frac{\partial^2 c_i}{\partial y^2} \right) \quad (25)$$

Equations (24) and (25) were discretized by a finite volume method. In each control volume the mass balance is:

$$F_{y_{up}} + F_{x_{left}} = F_{y_{down}} + F_{x_{right}} + \frac{dm}{dt} \quad (26)$$

where the letter F is used to represent the mass fluxes, Fig. 3, and m is the mass of fluid in the finite volume.

The convective flux (F_c) is defined by:

$$F_c = v c_i \quad (27)$$

and the diffusive flux by:

$$F_d = -D_i \frac{\partial c_i}{\partial y} \quad (28)$$

To assure mass conservation, the pseudoconvective terms were discretized by the donor-cell upwind method [14].

Boundary conditions were introduced in the discretized equations of the finite volumes by considering the appropriate boundary fluxes or concentrations. At the membrane surface, the pseudoconvective flux at the membrane surface is zero:

$$F_{y_{down}} = 0 \quad (29)$$

and the pseudoconvective flux at the symmetric axis is also zero:

$$F_{y_{up}} = 0 \quad (30)$$

At the cell inlet the normalized concentration of both components are equal to 1:

$$c_i = 1 \quad (31)$$

and, at the cell outlet, the variation of the normalized concentration is equal to zero:

$$\frac{\partial c_i}{\partial x} = 0 \quad (32)$$

At membrane surface the diffusive flux down is equal to zero:

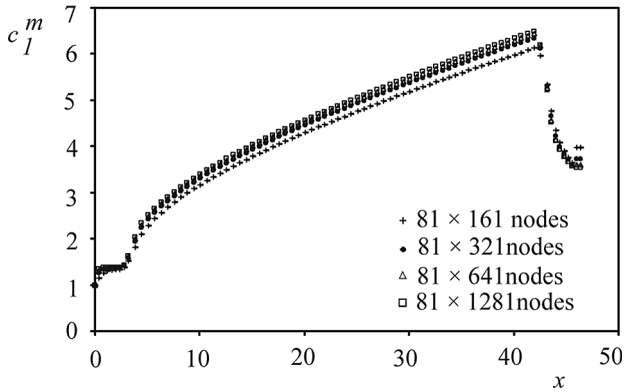


Fig. 4. Normalized concentration along the membrane surface for several grids for $Pe = 1 \times 10^5$, $\Delta P_0 = 1 \times 10^4 \text{ Pa}$, $V_0 = 5.7 \times 10^{-3} \text{ ms}^{-1}$, $\Pi_2 = 1.36 \times 10^6$, $\Pi_3 = 0.39$, $\phi_w = -10 \text{ mV}$ and $z = 1$.

$$F_{y_{\text{down}}} = 0 \quad (33)$$

as well as the diffusive flux up at the symmetric axis:

$$F_{y_{\text{up}}} = 0 \quad (34)$$

The diffusive flux left at cell inlet is also equal to zero

$$F_{x_{\text{left}}} = 0 \quad (35)$$

as well as the diffusive flux right at cell outlet:

$$F_{x_{\text{right}}} = 0 \quad (36)$$

5.1. Validation of the numerical code

The numerical code developed to solve the mass transport equation is a new code that needs to be validated. The validation can be accomplished by comparing the solution obtained with the code for a cell with stagnant fluid with the theoretical prediction given by the Boltzmann equation. The concentration profile, given by the Boltzmann equation, is:

$$c_i = c_0 \exp[-z_i \Pi_3 (\phi - \phi_0)] \quad (37)$$

5.2. Grid optimization

Grid tests were performed to select the best grid to perform the simulations (Fig. 4). The result obtained for grid 81×671 is almost the same as the one obtained for the grid $81 \times 1,281$. Therefore, error associated with a grid with 81×641 nodes is very small and so this was the grid selected.

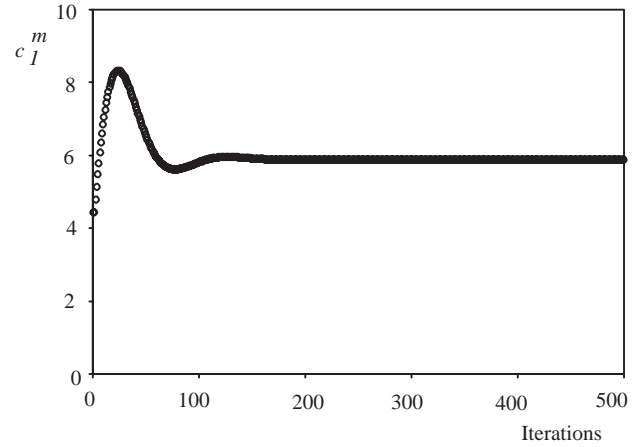


Fig. 5. Normalized concentration in a critical node near the end of the cell versus the number of iterations for $Pe = 1 \times 10^5$, $\Delta P_0 = 1 \times 10^4 \text{ Pa}$, $V_0 = 5.7 \times 10^{-3} \text{ ms}^{-1}$, $\Pi_2 = 1.36 \times 10^6$, $\Pi_3 = 0.39$, $\phi_w = -10 \text{ mV}$ and $z = 1$.

5.3. Convergence

The study of the convergence of the numerical method was based on the error in the concentration of the solutes in a critical node of the cell. The critical node is located near the cell exit, where the convergence is slower. The error of the concentration in the critical node was determined by:

$$\varepsilon_{\text{crit}} = \left| \frac{C_{\text{crit}}^k - C_{\text{crit}}^{k-1}}{C_{\text{crit}}^k} \right| \quad (38)$$

where crit refers to the critical node and k to the current iteration.

An example of the study of the convergence is presented in Fig. 5. The normalized concentration converges to a constant value. The iterative process stops when the following criterions were observed:

$$\varepsilon_{\text{crit}} < 10^{-3} \quad (39)$$

6. Results and discussion

The electric potential equation was solved to determine the electric field in the membrane cell. The results, for two values of the membrane potential are in Fig. 6. The data show that the membrane disturbs the electric field along a short distance of 0.05 H.

The introduction of the electric field requires the validation of the numerical method implemented. The numerical method was validated by comparing data obtained for a stagnant fluid with the Boltzmann equation. The comparison is shown in Figs. 7 and 8. The results obtained by the numerical method are accurate, even for large membrane potentials.

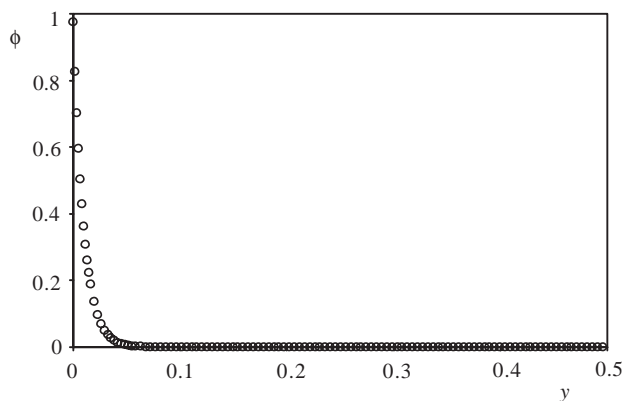


Fig. 6. Normalized potential along the direction normal to the membrane for $\Pi_2 = 1.36 \times 10^6$ and $\Pi_3 = 0.39$.

The separation process was studied considering two membrane cells: a neutral membrane cell and a negatively charged membrane cell. The results are in Fig. 9. Fig. 9 shows that the concentration along the membrane is higher when the membrane and the component have opposite charges and lower when the membrane and the component have the same charge. Both components have the same intermediate concentration in the cell with a neutral membrane.

7. Conclusions

The Poisson-Boltzmann, the Nernst-Planck equation and the Navier-Stokes equations were solved by numerical methods to study the mass transport of charged species in the vicinity of a charged membrane. The fractional-step method used to solve the mass transport equation is sufficiently adequate and easy to implement. The donor-cell upwind method used to discretize the convective terms of the mass transport equation assures mass conservation. The method to solve the mass

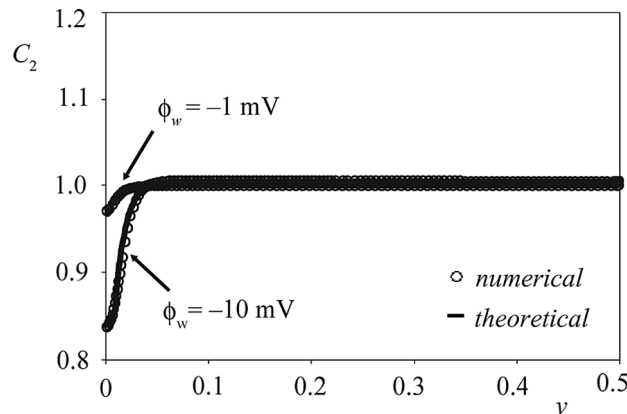


Fig. 8. Normalized concentration along the vertical direction of the species with a negative charge in a cell containing stagnant fluid for $\Pi_2 = 1.36 \times 10^6$ and $\Pi_3 = 0.39$.

transport equation was validated by comparing the numerical solution for a membrane cell containing stagnant fluid with the Boltzman equation.

The code developed was used to study the mass transfer of two charged species in the vicinity of a semi-permeable negatively charged membrane. As it was expected, the ion with positive charge accumulates, in a higher quantity, near the membrane.

Further work is necessary to improve the code developed. In the future we intend to solve the full vorticity equation, including electric terms neglected in this work. The electric potential equation will be solved considering the effect of convection in the charged species distribution. Finally, the code will be improved to include a higher number of charged species, an improvement that will allow the study of protein fractionation.

Acknowledgments

The authors gratefully acknowledge the financial support of Fundação para a Ciência e Tecnologia (FCT)

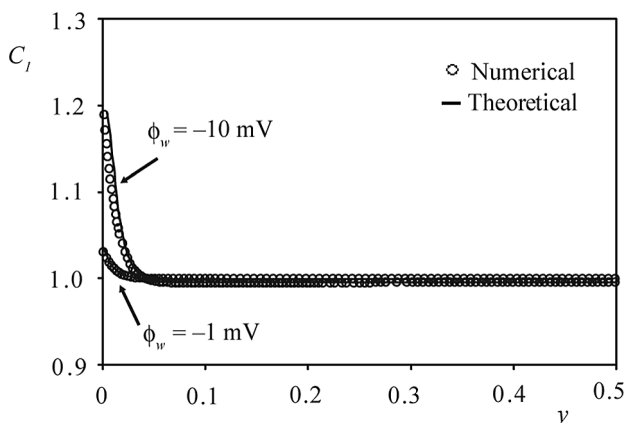


Fig. 7. Normalized concentration along the vertical direction of the species with a positive charge in a cell containing stagnant fluid for $\Pi_2 = 1.36 \times 10^6$ and $\Pi_3 = 0.39$.

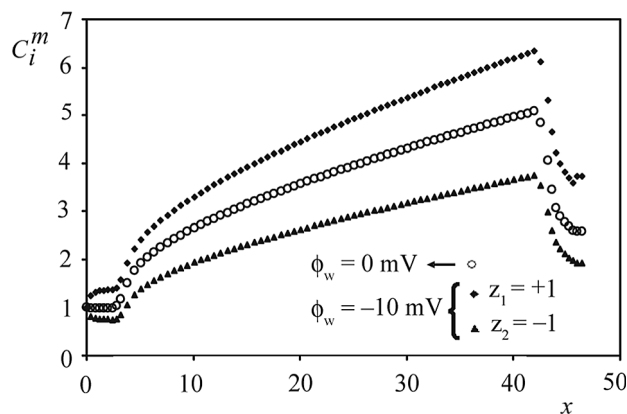


Fig. 9. Concentration along the membrane for $Pe = 1 \times 10^5$, $\Delta P_0 = 1 \times 10^4 Pa$, $V_0 = 5.7 \times 10^{-3} ms^{-1}$, $\Pi_2 = 1.36 \times 10^6$, $\Pi_3 = 0.39$, $\phi_w = 0$ and $\phi_w = -10 mV$ ($z_1 = 1$ and $z_2 = -1$).

through project POCI/EQU/59724/2004 and scholarship SFRH / BD / 27821 / 2006. POCTI (FEDER) also supported this work via CEFT.

Symbols

C_i	Solute concentration of component i
c_i	Normalized solute concentration of component i
C_0	Ionic feed/bulk concentration
C_0^+	Normalized ionic feed/bulk concentration
C_0^+	Concentration of the positively charged component
C_0^-	Concentration of the negatively charged component
C_i^m	Concentration of component i at membrane surface
c_i^m	Normalized solute concentration of component i at membrane surface
C_{crit}^k	Concentration on a critical location
D_i	Molecular diffusivity of component i
F	Faraday constant
F_c	Convective mass flux
F_d	Diffusive mass flux
$F_{y_{down}}$	Mass flux across the lower boundary of a finite volume
$F_{y_{up}}$	Mass flux across the upper boundary of a finite volume
$F_{x_{left}}$	Mass flux across the left boundary of a finite volume
$F_{x_{right}}$	Mass flux across the right boundary of a finite volume
H	Distance between parallel plates
k	Current time step
L_{out}	Length of the outlet section
L_{in}	Length of the inlet section
L_m	Total length of the membrane
L	Length of the cell
M	Molar mass
R	Gas constant
r_e	Normalized ionic concentration
R_m	Membrane resistance
T	Temperature
T	Non-dimensional time
V_0	Mean feed velocity
V_x	Longitudinal component of the velocity
v_x	Normalized longitudinal component of the velocity
\hat{v}_x	Normalized pseudovelocity (component x)
V_y	Vertical component of the velocity
v_y	Normalized vertical component of the velocity
\hat{v}_y	Normalized pseudovelocity (component y)
X	Longitudinal coordinate

x	Normalized longitudinal coordinate
Y	Vertical coordinate
y	Normalized vertical coordinate
W	Width of the cell
z_i	Charge of component i

Non-dimensional numbers

Pe	Peclet number
Re	Reynolds number
Π_1	Non-dimensional number defined by Eq. (12)
Π_2	Non-dimensional number defined by Eq. (2)
Π_3	Non-dimensional number defined by Eq. (5)

Greek symbols

ΔP_0	Static pressure difference across the permeable membrane
ε	Permittivity
ε_{crit}	Numerical error of the concentration on a critical location
ψ	Stream function
ω	Vorticity
ρ	Density
μ	Viscosity
Φ	Electric potential
ϕ	Non-dimensional electric potential
Φ_0	Electric potential of the bulk
ϕ_0	Normalized electric potential of the bulk
Φ_w	Membrane electric potential
ϕ_w	Normalized membrane electric potential

References

- [1] R. Gosh, Protein Bioseparation Using Ultrafiltration | Theory, Applications and New Developments, Imperial College Press, London, 2003.
- [2] C.H. Müller, G.P. Agarwal, Th. Melin and Th. Wintgens, J. Membr. Sci., 227 (2003) 51–69.
- [3] Q.Y. Li, Z.F. Cui and D.S. Pepper, J. Membr. Sci., 136 (1997) 181–190.
- [4] W. Richard Bowen, Meirion G. Jones and Haitham N.S. Yousef, Chem. Eng. Sci., 53 (1998) 3793–3802.
- [5] S. Bhattacharjee, Albert S. Kim and M. Elimelech, J. Colloid Interface Sci. 212 (1999) 81–99.
- [6] M. Nystrom, P. Aimar, S. Luque, M. Kulovaara and S. Metsamuuronen, Colloids Surf. A Physicochem. Eng. Aspects, 138 (1998) 185–205.
- [7] S. Saksena and A.L. Zydney, J. Membr. Sci., 125 (1997) 93–108.
- [8] W.R. Bowen and Paul M. Williams, Chem. Eng. Sci., 56 (2001) 3083.
- [9] S. Ma, S.C. Kassinos and D. Kassinos, J. Membr. Sci. 337 (2009) 81–91.
- [10] S.I.S. Pinto, T.M.G.T. Rocha, J.M. Miranda and J.B.L.M. Campos, Desalination, 241 (2009) 372–387.
- [11] R. Gosh and Z.F. Cui, J. Membr. Sci., 180 (2000) 29–36.
- [12] W.S. Opong and A.L. Zydney, AIChE J., 37 (1991) 1497–1510.
- [13] A. Martín, F. Martínez, J. Malfeito, L. Palacio, P. Prádanos and A. Hernández, J. Membr. Sci., 213 (2003) 225–230.
- [14] Randal J. Leveque, Finite Volume Methods for Hyperbolic Problems, Cambridge University Press, New York, 2003.